Characterization of UWB Transmit-Receive Antenna System

Alireza H. Mohammadian†, Amol Rajkotia, and Samir S. Soliman

QUALCOMM Incorporated, 5775 Morehouse Drive, San Diego, CA 92130
†E-mail: ahm@qualcomm.com

***Abstract* – An ultra-wide-band (UWB), stripline-fed Vivaldi antenna is characterized both numerically and experimentally. Three-dimensional far-field measurements are conducted and accurate antenna gain and efficiency as well as gain variation versus frequency in the boresight direction are measured. Using two Vivaldi antennas, a free-space communication link is set up. The impulse response of the cascaded antenna system is obtained using full-wave numerical electromagnetic time-domain simulations. These results are compared with frequency-domain measurements using a network analyzer. Full-wave numerical simulation of the free-space channel is performed using a two step process to circumvent the computationally intense simulation problem. Vector transfer function concept is used to obtain the overall system transfer function and the impulse response.**

I. INTRODUCTION

Unlike narrowband systems, the antenna plays an integral role in an UWB system. UWB systems transmit extremely narrow pulses on the order of 1ns or less resulting in bandwidths in excess of 1 GHz. From a system design perspective, the impulse response of the antenna is of particular interest because it has the ability to alter or shape the transmitted or received pulses. If one were to design a matched filter receiver, a clear understanding of the shape of the pulse at the receiving antenna terminals is needed. Hence, the cascaded response of the transmitting (TX) and receiving (RX) antennas play a key role in shaping the pulse.

In several papers on UWB, it has been claimed that the voltage received at the RX antenna terminals is the second derivative of the excitation voltage at the TX antenna terminals. For example, a Gaussian pulse exciting a TX antenna would be transformed to its second derivative when observed at the RX antenna terminals. In fact, this assumption has been used in most papers to design the template waveform for a correlator- (matched-filter-) based receiver.

The relationship between the input voltage/current of a TX antenna and the field it generates is a function of several parameters including the antenna geometry, material, current mode, and the transmitter impedance. In general, this relationship does not hold a fixed form (derivative, double derivative, etc.) and is dependent on these parameters. The same is true for the relationship between the incident field and the received voltage/current for an RX antenna. That is also true for the terminal voltages (or currents) of a TX-RX antenna system. To claim that for an UWB system, the received voltage is always the first or second derivative of transmitted voltage is incorrect. The myth may have been stemmed from an extrapolation of some early research works on the transient behavior of linear antennas. For example, it may be shown [1] that if a pulse excites a dipole much shorter than the wavelength of the highest frequency in that pulse, the radiated field is proportional to the first or second derivative of the pulse depending on whether the current distribution is assumed traveling or standing. It is not an inherent property of the UWB signals or system that the output is always the first or second derivative of the input. We will address this issue in a future correspondence.

Ideal antennas used in an UWB TX-RX system should faithfully replicate the transmitted pulse at the receiving end. In practice, attempt must be made to limit the amplitude and group delay distortion below certain threshold that will ensure reliable system performance.

The purpose of the current study is to establish a full-wave numerical simulation approach for the characterization of an UWB TX-RX antenna system in an attempt to design better receivers. The predicted impulse response and transfer function of the system is compared to the measured results to prove the validity of the numerical approach. The Vivaldi antenna chosen here merely serves as an example to show the characterization methodology. This antenna, while providing an adequate bandwidth for the UWB spectrum, may not necessarily be the optimum choice for every UWB system. In Section II, we discuss the numerical approach used to characterize an individual antenna, followed by a post-processing stage to create a model for a free-space link with two antennas. The transfer function and impulse response of this link is then derived. In Section III, our measurement method will be explained leading to an experimental evaluation of the transfer function and impulse response of our free-space link. Finally, in Section IV, the numerical and experimental results are compared and some conclusions are derived.

II. FULL-WAVE NUMERICAL APPROACH

Electromagnetic (EM) simulation provides useful insight into the performance of the individual components of an UWB link, in particular the TX and the RX antenna. It also makes it more time and cost effective to investigate the effects of the antenna type and orientation on the UWB system performance through parametric studies. Traditionally, most EM simulations of antennas are limited to characterization of the antenna input impedance and far field gain patterns over a narrow band of frequencies. As such, an EM simulation tool in the frequency domain is often adequate and preferred. In our study of UWB antennas and UWB communication links, we characterize the antennas and the channel using system level concepts such as transfer functions and impulse responses. Therefore, EM simulation in the time domain is more appropriate. In the following analysis, the time-domain EM simulation tool Micro-Stripes [2] was used.

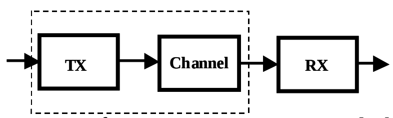

Fig. 1. Components of an UWB communication link.

The communication link is divided into two components (Fig. 1), the TX antenna and the channel as one segment, and the RX antenna as the other. The complete link is reconstructed in the post-processing stage.

A. Characterization of an Individual Vivaldi Antenna

A Vivaldi antenna is designed and its performance is optimized through full-wave numerical simulations. Two prototypes of this design measuring 90 mm by 40 mm by 3.15 mm were built on a two-layer Roger 5870 substrate (ε_r = 2.33, tanδ = 0.0016), and their return loss measured. (See Fig. 2.)

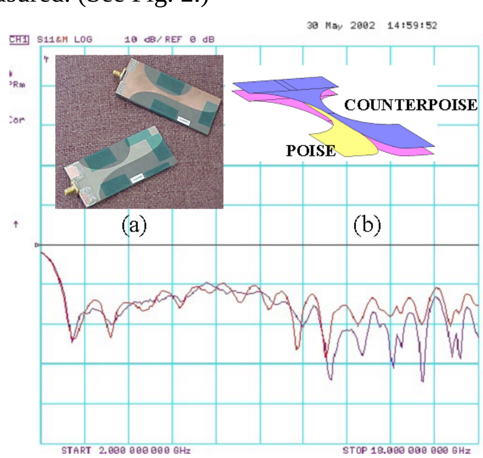

(c)

Fig. 2. (a) A picture of the UWB Vivaldi antenna prototypes. (b) Simulation geometry showing the internal details of the antenna. (c) Measured return loss for the two Vivaldi antennas.

As Fig. 2(b) shows, the top- and bottom-layer metallizations constitute the ground planes for the stripline feed and the counterpoise, while the mid-layer metallization, serves as the poise and the strip. Fig. 3 shows predicted and measured boresight gains versus frequency. The agreement between the predicted and measured gain values is very good over the entire UWB spectrum (i.e. 3.1 GHz ~ 10.6 GHz).

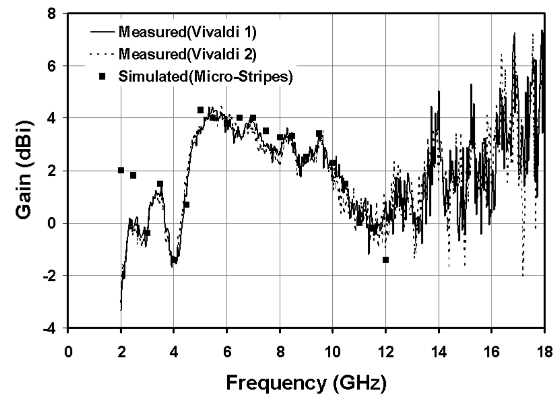

Fig. 3. Boresight gain versus frequency for the Vivaldi antenna.

B. Simulation of TX/Channel Segment

In the TX / Channel portion, the TX antenna is excited by an input pulse voltage and the time-domain fields are computed at a distance R (> $2D^2/\lambda$) from the antenna as depicted in Fig. 4. A full-wave simulation of Maxwell's equations in the time domain is performed and the observation point is extended to the far-field region.

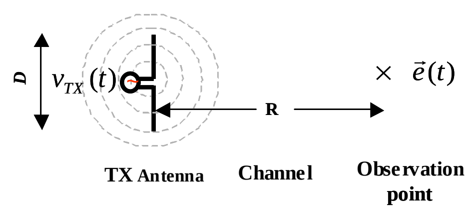

Fig. 4. TX-Channel portion of the UWB communication link

D is the characteristic dimension of the antenna and λ is the wavelength of the highest frequency in the pulse spectrum with non-negligible power.

C. Post-Processing of the TX Antenna / Channel Segment

The output and input signals are converted to the frequency domain using Fourier transformation.

A vector transfer function for the TX antenna/channel is defined relating the input voltage at the terminals of the TX antenna to the electric far field in the desired direction:

$$\vec{H}_{TX/Ch}(f) = \frac{\vec{E}(f)}{V_{TX}(f)}. \quad (1)$$

where $\vec{E}(f)$ and $V_{TX}(f)$ are the Fourier transform of the electric field $\vec{e}(t)$ and the input voltage $v_{TX}(t)$, respectively.

D. Simulation of the RX Antenna

A plane wave pulse with polarization $\hat{c}$ is incident upon the RX antenna from a direction parallel to the line that connects the phase centers of the TX and RX antennas as depicted in Fig. 5(a). In theory, an impulse is used to find the impulse response of a system. In numerical simulations, a pulse such as

$$g(t) = 2 f_c \operatorname{sinc}(2\pi f_c t) e^{-(\pi f_g t)^2} \tag{2}$$

may be used instead, provided the pulse amplitude in the frequency domain over the frequency band of interest remains nearly a constant. The parameters in (2) are given as f_c = 1.3 f_{op} and f_g = 0.2 f_{op} where f_{op} is the highest output frequency. This plane wave pulse generates a voltage across the terminals of the RX antenna that may be computed via a full-wave simulation of Maxwell's equations in the time domain.

E. Post-processing of the RX Antenna Simulation

In general, the sampling rates for the simulations of the TX and RX antenna are different. Therefore, it may become necessary to use zero padding and interpolation before calculating the transfer function in the post-processing stage. Once the sampling rates are identical, the Fast Fourier Transforms (FFTs) are utilized to find the frequency spectrum of the input and output quantities and derive a transfer function. The details are shown in Fig. 5(b) where tilde indicates original quantities. A vector transfer function for the RX antenna is now defined through the following vector expression:

$$V_{RX}(f) = \vec{E}(f) \cdot \vec{H}_{RX}(f). \tag{3}$$

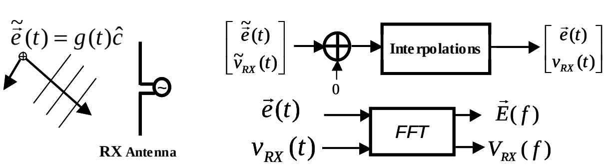

(a) (b)

Fig. 5. (a) A plane-wave pulse incident on the RX antenna. (b) Post-processing of the RX antenna input and output.

F. Transfer Function and Impulse Response of the Overall System

$\vec{E}(f)$ is substituted from (1) into (3) to establish a relationship between the excitation voltage at the TX antenna and the received voltage at the RX antenna. The transfer function between the TX and RX antenna may then be given by

$$H_{Link}(f) = V_{RX} / V_{TX} = \vec{H}_{TX/Ch}(f) \cdot \vec{H}_{RX}(f). \tag{4}$$

It is interesting to note that while the transfer functions of the TX antenna/Channel and the RX antenna are vector quantities, the transfer function of the link being the inner product of these two vectors is scalar since the input and output quantities are scalars.

The impulse response may be obtained by computing the inverse Fourier transform of the transfer function

$$h_{Link}(t) = \frac{1}{2\pi} \int_{-\infty}^{+\infty} H_{Link}(f) e^{i2\pi f} df. \tag{5}$$

III. MEASUREMENT METHOD

There are two different approaches for the impulse response measurements. The first is the direct time-domain approach using an extremely fast sampling oscilloscope. The second approach is to make the measurement in the frequency domain using a network analyzer. In the first method, the transmitting antenna is excited with an extremely narrow pulse and the received waveform is captured using an oscilloscope. If the exciting pulse bandwidth is much larger than the antenna system bandwidth, then the measured signal is a good approximation of the system impulse response. However, if the exciting pulse bandwidth is comparable to that of the antennas, then, a de-convolution process is required.

The second approach is to make the measurements in the frequency domain. Here, a network analyzer is used to measure the cascaded frequency response of the RX/TX antennas. The analyzer is swept from close to DC to about 12 GHz and the complex response of the system measured. This frequency data is then converted to the bandpass equivalent by taking the complex conjugate data and zero padding it where needed. The impulse response is then computed by taking the IFFT. The reason for choosing 12 GHz as the upper limit is because (a) the antennas are designed to operate below 10 GHz and (b) even if the antennas have high frequency gain, the rest of the receiver will most likely have a front-end interference rejection filter with a cut-off of 12 GHz or less. Detailed procedure for making this measurement is explained below and a block diagram of this approach is shown in Fig. 6. Mathematically, the cascaded impulse response can be computed as shown below.

$$H(f) = H_{TX}(f) H_{CH}(f) H_{RX}(f) = \frac{Y(f)}{X(f)} = S_{21} \tag{6}$$

$$h[n] = \operatorname{Re}\{IFFT[H(f)]\}$$

where *h[n]* is the impulse response computed using

IFFTs. Due to the lack of a fast sampling oscilloscope, we chose the second approach in making the measure-

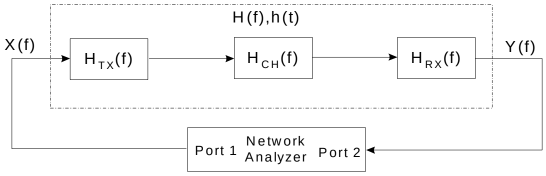

Fig. 6. Frequency Domain Measurement

ments. This is also the approach that has been taken by several researchers to model RF channels. [3, 4]

A. Impulse Response

The RX and TX antennas were placed in an anechoic chamber with sufficient horizontal separation to be in the far field of each other as shown in Fig. 7. The two antennas were oriented to boresight. The network analyzer frequency was swept in the desired range and the magnitude and phase of the RX/TX cascaded response were stored. This provided the complex scattering parameter S_{21}. Next, a conjugate reflected frequency response S^*_{21} was formed and with appropriately zero padding the data, arrived at the final frequency response vector, which is called *H(f)*. The impulse response *h[n]* was obtained by taking the real part of the IFFT of *H(f)*. The above procedure was repeated for various orientations of the RX antenna.

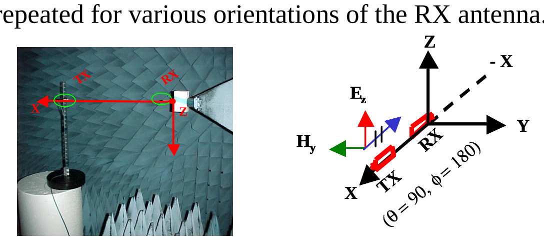

(a) (b)

Fig 7. (a) Free-space UWB link inside an anechoic chamber. (b) TX and RX antenna and the direction of propagation.

B. Antenna FIR model from impulse response

We took the impulse response samples that contain more than 97% of the power. This is given by the following expression:

$$100 * \sum_{n=n1}^{n2} h^2[n] / \sum_{n=1}^{N} h^2[n] \geq 97 \tag{7}$$

where N is total number of points in the impulse response, and n_1,n_2 are sample indices of window that contains 97% of the power. The samples from n_1 to n_2 are chosen as the coefficients of the FIR filter used to model the cascaded RX/TX antenna.

When different antenna orientations are used, the above method may sometimes give different number of coefficients. Thus, to be consistent in the simulation by utilizing exactly the same size FIR filter, all samples between 2ns and 6ns were chosen as the FIR coefficients. This 4ns window contained more than 99% of the power.

C. Group Delay

A good measure of the performance of a filter is its group delay, defined as the negative derivative of the filter phase with respect to frequency. When a signal passes through a filter, it experiences both amplitude and phase distortion. The amount of distortion depends on the characteristics of the filter. A waveform incident at the input of a filter may have several frequency components. The group delay gives an indication of the average time delay the input signal suffers at each frequency. Stated differently, this parameter gives an indication of the dispersive nature of the filter. Mathematically, the filter response and group delay are given by:

$$H(f) = A(\omega) e^{j\theta(\omega)}; \qquad \tau_g = -\frac{d\theta(\omega)}{d\omega}. \tag{8}$$

If the filter has a non-linear phase response, the group delay will vary with frequency causing the input signal to experience different delays at different frequencies. As a result, the output waveform is likely to be distorted. For a filter to be linear phase (have constant group delay), its phase response must satisfy one of the following relationships:

$$\theta(\omega) = -\alpha\omega; \qquad \theta(\omega) = \beta - \alpha\omega. \tag{9}$$

It can be shown that in order to satisfy either one of the above conditions of linear phase, the impulse response of an FIR filter must have positive or negative symmetry [5]. The simulation results of the previous section shows that the antenna does not possess this symmetry.

The UWB antenna can be viewed as a filter with some magnitude and phase response. By representing the Rx/Tx antenna system as a filter, we can determine its phase linearity within the frequency band of interest by looking at its group delay. The phase response and group delay are related to the antenna magnitude (gain) response. For example, if there is a null in the magnitude, it implies a nonlinear phase, and therefore, a non-constant group delay. Unless there are large variations in the magnitude, it is difficult to determine the phase linearity by simply looking at the phase plots. The group delay plot is able to clearly show any non-linearity that may be present in the phase. The pulse input to the antenna system has an extremely large bandwidth and hence, any variation in group delay across the pass band of the transmitted pulse is likely to distort the pulse. To characterize the antenna, the peak-to-peak variations of the gain and group delay within the 10dB bandwidth of the input pulse is determined.

IV. RESULTS

The UWB antenna was characterized for different orientations of the receiving antenna. The RX antenna was positioned at elevations of α = -135, -90, -45, 0, 45, 90, 135 degrees for each of the azimuths of β = 0, 90, and 135 degrees to give a total of 21 orientations. The elevation angles correspond to the rotation of the RX antenna pedestal in the horizontal plane, while the

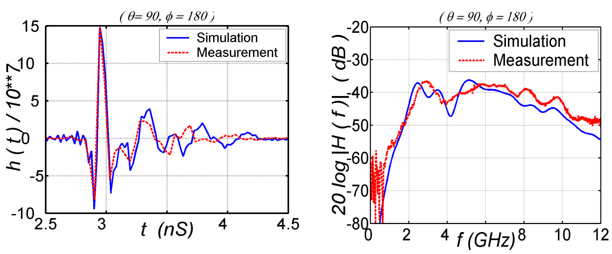

(a) (b)

Fig. 8. (a) Impulse response and (b) transfer function corresponding to the case α = 0°, and β = 0° in Table 1.

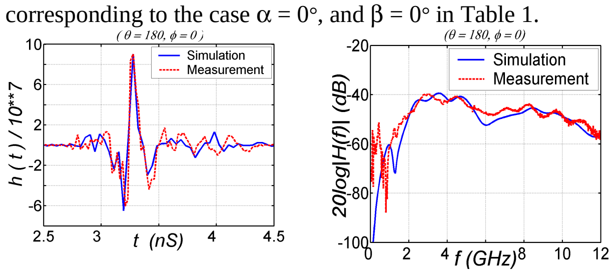

(a) (b)

Fig. 9. (a) Impulse response and (b) transfer function corresponding to the case α = 90°, and β = 0° in Table 1.

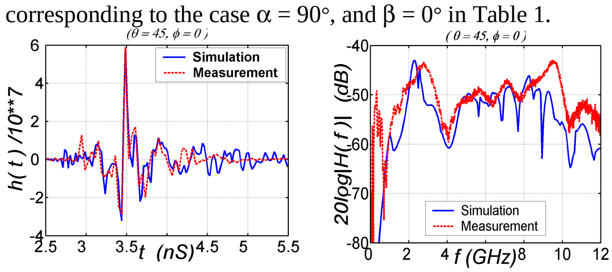

(a) (b)

Fig. 10. (a) Impulse response and (b) transfer function corresponding to the case α = 135°, and β = 0° in Table 1.

azimuth angles correspond to the orientation of the TX antenna on a fixed stand. The convention used for the numerical simulations indicated on the figures (i.e., θ, ϕ) is based on the direction of the waves propagating from the TX antenna toward the RX antenna, which is always fixed at its position as indicated in Fig. 7(b). Some typical results are shown in Fig. 8 to Fig. 10. It should be noted that the system noise floor for these measurements was less than –75 dB.

Table 1 indicates that for β = 0 degrees, the peak to peak group delay variation measured in 4.32 GHz to 5.68 GHz (10dB incident pulse bandwidth of 1.36 GHz) is relatively small, ranging from about 7 to 17 samples for different α. The gain variation within the same bandwidth is found to be about 3 dB to 11.6 dB. In contrast, a large variation is seen when β = 90 degrees, where the group delay varies from 19 to 42 samples and the gain varies from 5 dB to 17 dB. Thus, the 90-degree azimuth case will distort the incident signal the most.

Table 1. Antenna group delay and gain variation

	τ_g Variation (samples)			Gain Variation (dB)		
α↓,β→	0°	90°	135°	0°	90°	135°
UWB Vivaldi Antenna (variations within 4.32 to 5.68 GHz.)						
-135°	16.8	42	27.7	11.6	17.2	4.9
-90°	7.6	20.5	20.3	5.5	11.6	9.3
-45°	13.9	28.3	18.2	3.4	9.1	7.2
0°	7.6	18.8	16.8	4.4	7.7	5
45°	11.3	19	15.3	3.3	10.1	6.6
90°	12.6	22.5	15.8	6.6	12.6	9.4
135°	16.4	38.9	15.8	7.4	5.2	7.3

V. CONCLUSIONS

A time-domain simulation method of characterizing UWB TX-RX antenna systems was presented in this paper. The measured antenna transfer function was found to be close to the simulated one indicating that we can use a software-based approach to determine an antenna model for most orientations. From the cascaded impulse response, the received waveform can easily be determined for any arbitrary incident pulse. Since the incident signal bandwidth is in excess of 1 GHz, the group delay and gain variation across the entire bandwidth has to remain relatively flat to prevent signal distortion. Further measurement on an omni-directional antenna need to be performed to validate the effect of gain and group delay on the receiver performance. In general, obtaining an antenna with flat gain and group delay variation across multi-gigahertz and across different angles is non-trivial and the received waveform will be very sensitive to antenna motion.

REFERENCES

[1] D. L. Sengupta and C.-T. Tai, "Radiation and reception of transients by linear antennas," *Transient Electromagnetic Fields*, L. B. Felsen, Eds., Springer-Verlag, 1976.

[2] *Micro-Stripes Reference Manual*, Release 6, Flomerics Ltd., Surrey, UK.

[3] S.J. Howard and K. Pahlavan, "Measurement and analysis of the indoor radio channel in the frequency domain," *IEEE Transactions on Instrumentation and Measurement*, vol. 39, Oct. 1990.

[4] S. Ghassemsadeh, V. Tarokh, C.W. Rice, W. Turin, R. Jana, " A statistical path loss model for in-home UWB channels," *Digest of the 2002 IEEE Conference on Ultra Wideband Systems and Technologies*, pp. 59-64.

[5] E. C Ifeachor, B.W Jervis, *Digital Signal Processing, A practical Approach*, Addison-Wesley, 1993.